

Available online at www.sciencedirect.com**ScienceDirect**

Procedia CIRP 36 (2015) 279 – 284

www.elsevier.com/locate/procedia

CIRP 25th Design Conference Innovative Product Creation

Design of Porous Micro-Structures using Curvature Analysis for Additive-Manufacturing

Yizhak Ben Shabat*, Anath Fischer

Faculty of Mechanical Engineering, Technion, Haifa 32000, Israel

* Corresponding author. Tel.: +972-48292334; E-mail address: sitzikbs@tx.technion.ac.il

Abstract

The emerging field of additive manufacturing with bio-compatible materials has led to personalized design of porous micro-structures used in healthcare. Complex micro-structures are characterized by freeform surfaces and spatially varying porosity. Currently, there is no CAD system that can handle the design of micro-structures due to their high complexity. This paper describes a direct expansion of our research on *generating 3D adaptive models of porous micro-structures*. Using this approach, a designer can either manually select a Region of Interest (ROI), or define a curvature based criterion for selecting ROI while defining its level of detail. In the proposed approach, the multi-resolution volumetric model is based on designing a customized model, composed of the following stages (a) Reconstructing a multi-resolution volumetric model of a porous structure; (b) Defining ROIs and their resolution properties; and (c) Constructing an adaptive model. The feasibility of the proposed method is demonstrated on 3D models of porous micro-structures. These models are characterized by a large amount of detail and geometrical complexity. The proposed method has been applied on bone models that were reconstructed from micro-CT images. The proposed approach facilitates the porous characteristic and enables local reduction of the model complexity while optimizing the accuracy. For additive manufacturing application, the approach can be used for designing a porous micro-structure with reduced material volume while eliminating irrelevant geometric features.

© 2015 The Authors. Published by Elsevier B.V. This is an open access article under the CC BY-NC-ND license

(<http://creativecommons.org/licenses/by-nc-nd/4.0/>).

Peer-review under responsibility of the scientific committee of the CIRP 25th Design Conference Innovative Product Creation

Keywords: multi-resolution modeling; personalized design; porous micro-structures; bone scaffolds; Design for additive manufacturing

1. Introduction

Multi-resolution volumetric modeling is applied in a variety of fields, including additive manufacturing, computer vision, virtual reality, finite element analysis and CAD. In recent years the significance of multi-resolution modeling has increased due to the ability of creating highly detailed models. It increases the effectiveness of computation, transmission, storage and visualization of the geometric model. Visualizing a high resolution model is time consuming and requires high computer resources. In order to cope with this challenge an adaptive method is required. It enables to select Regions of Interest (ROI) with desired

resolutions. In this manner an artificial fusion between different resolutions is generated.

Volumetric hierarchical representations allow a bi-directional transition from a macro-resolution model to a micro-resolution model. The most common hierarchical multi-resolution data structures for 2D images and 3D volumes are Quadtree and Octree, respectively. Their main principle is the recursive decomposition of space by a factor of two for each axis [1, 2]. These data structures are also compatible for methods which generate adaptive multi-resolution models. The ROI selection process can be either manual or based on geometric properties.

In the field of computer graphics and CAD, the geometrical characteristics of surfaces play an important role in many applications such as: feature extraction and suggestive contouring. Curvature is one of the most important surface characteristic. For continuous representation of parameterized surfaces the challenge of deriving shape characteristics can be expressed in a closed form formula of differential geometry. However, for discrete surfaces, represented as volumetric voxel model or by a triangular mesh, an approximation must be made. For volumetric voxel models, to the best of our knowledge, there is no direct method that approximates the voxel curvature. Therefore, in order to approximate the curvature, first the underlying surface must be approximated.

2. Approach

In this research the representation method for Quadtree and Octree proposed by Gargantini [3] has been used. The result of this method is a structure, from which the path to each node along the hierarchy can be extracted. The hierarchical nature of the tree structure is based on an explicit representation of hierarchical levels of detail. The lowest level of detail is the root of the tree. The highest level of detail is the leaves of the tree. An extension of Podshivalov et al approach [4-6] was made, generating the hierarchical structure in a bottom-up approach and storing each level of detail separately. A mask field was introduced for each node and was populated after selecting a region of interest (ROI). The Area of Interest (AOI) was defined in an image, while the Volume of Interest (VOI) was defined in a volume. The mask was populated only for nodes that are inside the ROI. The mask represents the level of detail (LOD) for each node. This mask is the base for an adaptive method and enables the visualization of nodes from multiple levels according to the ROI.

When generating a new upper level there is a need to preserve the mask by finding the nonzero minimum of the mask value from all child nodes and storing it in the ancestor node. This method ensures that if a part of an ancestor is required to be at a certain LOD then each of its children will be accordingly displayed at the maximum allowed LOD. An outline of the adaptive method in the form of a block diagram is depicted Fig. 1

The approach is not limited in the aspect of ROI geometry or the LOD distribution. In previous work [7] four manual, user defined ROIs, were introduced: a) rectangular AOI with a constant LOD; b) circular AOI with a linear change of LOD between center and circumference; c) cuboid VOI with constant LOD; and d) spherical VOI with linear change of LOD between center and bounding surface.

In this work, an ROI selection criteria based on surface curvature is proposed. For volumetric voxel models there is no direct method to approximate the voxel curvature. Therefore, in order to approximate the curvature, first the underlying surface is typically approximated. The

"marching cubes" algorithm [8] was used for approximating the underlying surface as a triangular mesh. A fairing algorithm [9] was then used to smooth the stair like affect created when approximating the volumetric representation as a triangle mesh. Finally, Rusinkiewicz curvature estimating algorithm [10] was used to retrieve the curvature tensor and principal curvature in each vertex. The curvature based ROI selection criterion is applied on each voxel. Visualization of the principal curvatures is performed using a color coding scheme. For each vertex in the mesh, the principal curvatures k_1 and k_2 were examined. Each vertex color is determined by a linear interpolation between nine pairs of control values. These control values correspond to all possible combinations, positive, zero and negative, of k_1 and k_2 . The result of the interpolation is depicted in Fig. 2. The color coding scheme was chosen this way in an effort to represent both principal curvatures in a single color map.

The calculation of levels of detail requires conversions and manipulations of the data in order to preserve topological information. The 2D and 3D space was defined according to definition 2.1 given by Kong [11], who describes the adjacency for elements which are full and elements which are empty in order to prevent topological paradoxes. The topological preservation process uses the image shrinking algorithm described by Jia et al [12]. The algorithm examines the effect of changing a node's B/W color on the connectivity of its surrounding node neighbours. Fundamentally, this introduces an additional B/W color constraint in images and volume constraint for 3D models when traversing from a higher resolution to a lower one. Finally, the processed model undergoes through a visualization stage where hexahedral faces are drawn on a 2D plane or in a 3D space. The size of the faces is determined by its LOD parameters. This process results in an adaptive model.

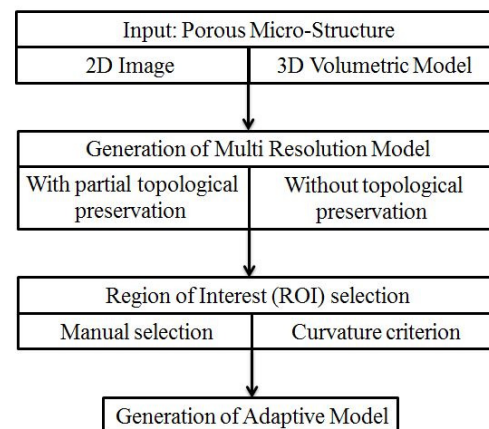


Fig. 1. Block diagram of the adaptation method

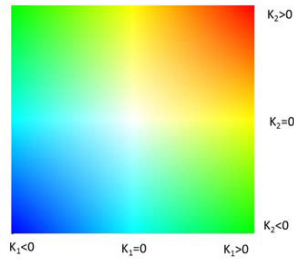


Fig. 2. Principal curvature color coding scheme of the proposed method

3. Examples and discussion

3.1. 2D Examples – Adaptive Models

In Fig. 3 the 2D result models of the approach using manual selection is presented [7]. Fig. 3 (a-e) depicts a synthetic 2D equivalent for a porous microstructure in the form of uniformly distributed circular holes in a 128x128 image. The AOI is marked by a circle of 64 pixels radius placed in the center of the image. The AOI properties are defined to be the maximum resolution in the center of the circle and change linearly to the minimum resolution on the circles circumference. The final model contains 8 levels of detail. However only levels of detail 1-5 are presented since levels 6-8 are redundant. Fig. 3 (f) presents the image fourth level of detail without the AOI for reference. Note that black pixels represent the presence of material and white pixels represent its absence.

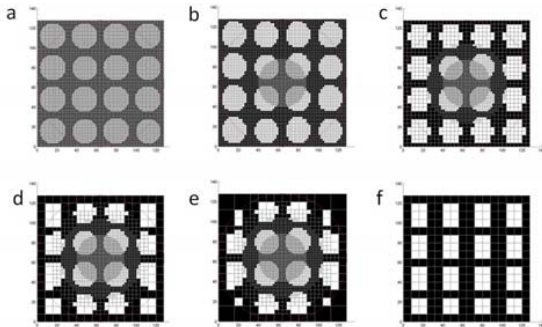


Fig. 3. Adaptive model 128X128 images with a circular linearly varying AOI. (a) Level one (input model), (b-e) levels two to five respectively, (f) level four of the same input without AOI for reference

3.2. 3D Examples – Curvature Analysis

Here we used a fragment of a slice of L3 vertebra model which was scanned using μ CT and digitized. The extraction of the fragment was performed by overlaying a 12x10 grid over the entire model. Each grid element is a 128^3 cube of voxel data which was processed separately. The extraction of these cubes was performed for computational speed and memory consumption reasons. Note that the entire original

high resolution vertebra model requires approximately 1 GB of memory only for its volumetric representation. Furthermore, a database for computational applications will require much more memory, for example, in finite element analysis the memory increases as a function of the problems degrees of freedom for each node. In Fig. 4 the extraction process is illustrated.

Fig. 5 depict the results of the curvature analysis which was applied on a bone fragment micro structure. Fig. 6 provides a zoomed in detailed view on some ROIs such as valleys (indicated in blue), ridges (indicated in red) and holes (indicated in green).

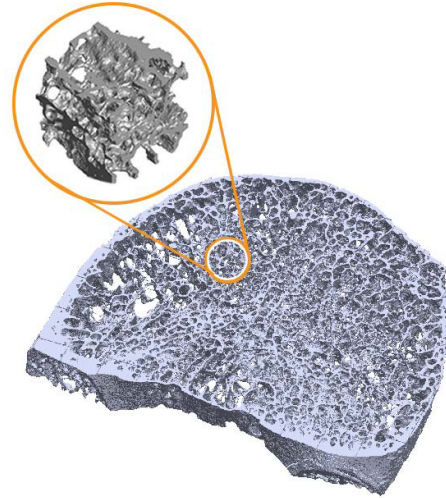


Fig. 4. Extraction of a 1283 cube from a slice of L3 vertebra

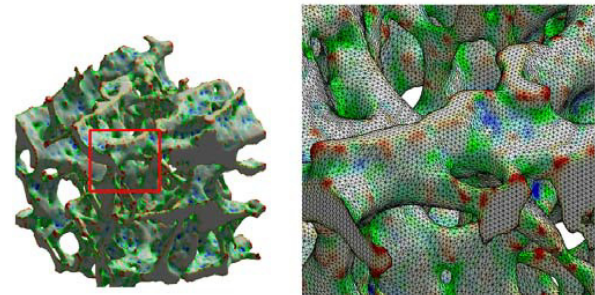


Fig. 5. Color coded curvature analysis of a bone fragment micro structure. Left – bone fragment, right – enlarged area with visible triangle mesh

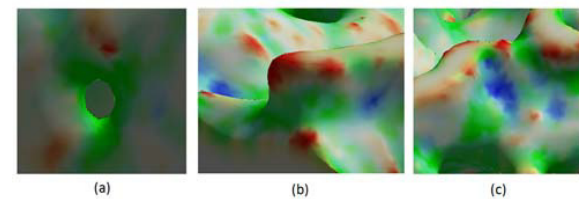


Fig. 6. Curvature analysis color coded ROIs (a) Local hole, (b) Local ridge, (c) Local valley

3.3. 3D Examples – Topological Preservation

The main effect of topological preservation on a model is depicted in Fig. 7 which show an original model of a wireframe cube. Without topological preservation the wire frame cube model changes significantly, it generates eight connected components instead of the initial one. When using the topological preservation method there is only one connected component, yet the frame thickness increases.

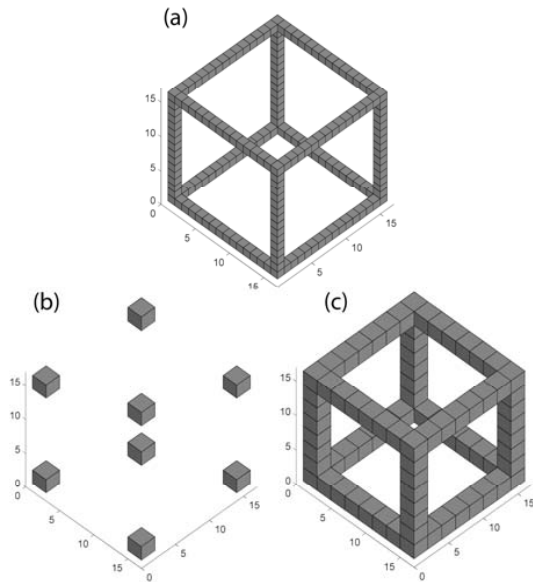


Fig. 7. Cube wireframe model. (a) Original model. (b) lower LOD without topological preservation. (c) lower LOD with topological preservation

Finally, the approach was applied on a bone fragment porous micro-structure. The effect of the topological preservation method on LODs 2-5 is depicted in Fig. 8. Since it is visually difficult to distinguish between the different connected components, they were colored differently. It is evident that when utilizing the topological preservation method there are significantly less components that disconnected from the main component.

A quantitative comparison of the connected components created using the two methods is presented in Fig. 9. The value for each LOD is the average and standard deviation over 20 different bone fragments. Both datasets converge to a single connected component in the lowest LOD. However, there is a significant difference (in 95% certainty) in LODs 3-5, indicating that when the topology is not preserved, a large amount of components get separated from the main component.

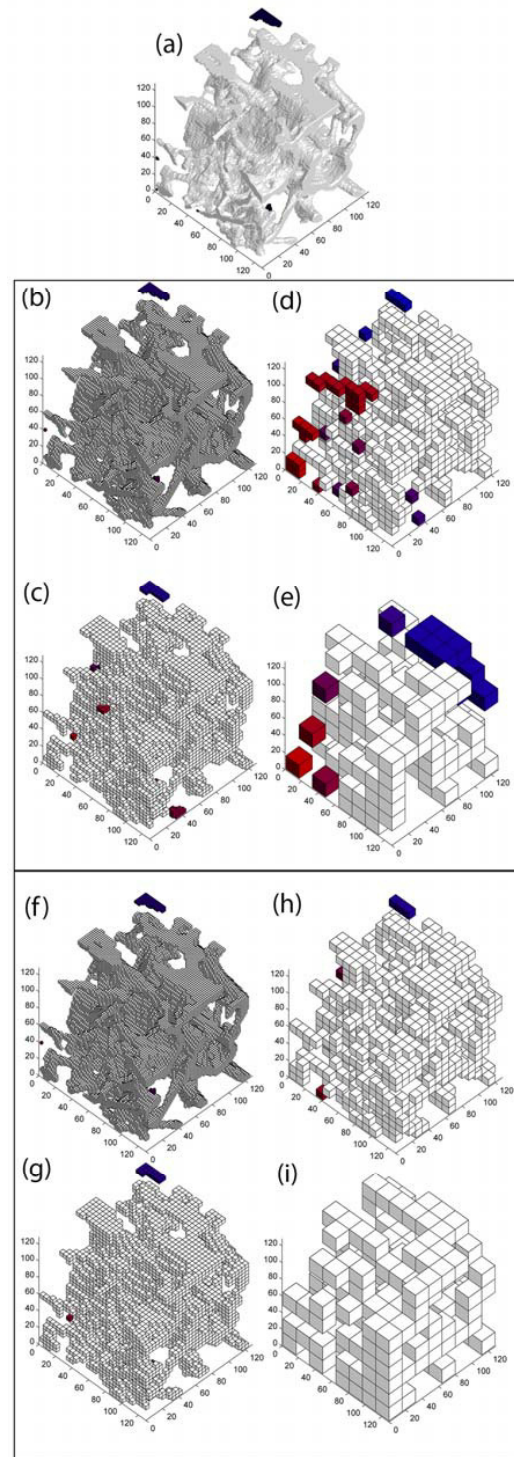


Fig. 8. 128^3 Bone porous micro-structure. (a) Original model (b-e) LODs 2-5 without topological preservation (f-i) LODs 2-5 with topological preservation

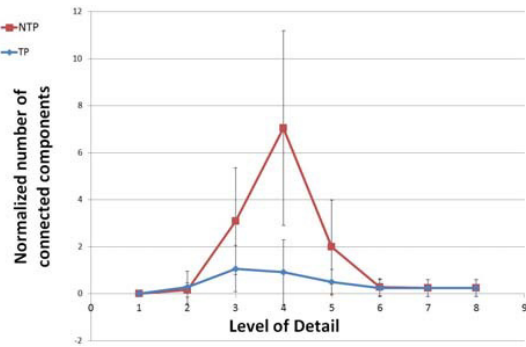


Fig. 9. Quantitative comparison of the normalized average number of connected components relative to the level of detail when using topological preservation method (TP) and not using topological preservation method (NTP). 20 bone fragments were used.

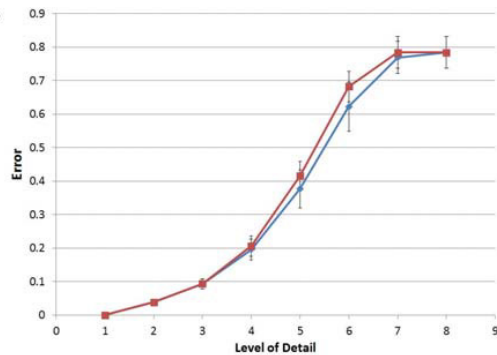


Fig. 10. Error comparison between non-topological preserved model (NTP) and a topological preserved model (TP) for $P_{Black} = P_{White} = 1$

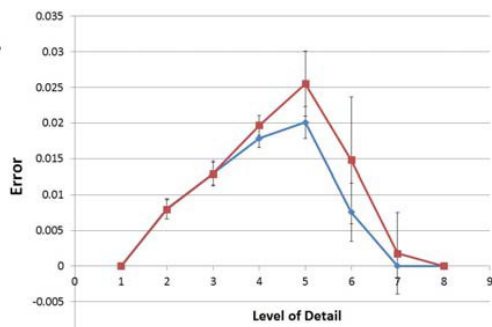


Fig. 11. Error comparison between non-topological preserved model (NTP) and a topological preserved model (TP) for $P_{Black} = 1, P_{White} = 0$

Furthermore, an analysis was performed for the volumetric error between the original model and each LOD. The error was subdivided into two main components:

- Black error ($error_{Black}$) – The relative portion of elements which were black in the original model and transformed to white in a lower LOD in relation to the entire volume.

- White error ($error_{White}$) – The relative portion elements which were white in the original model and transformed to black in a lower LOD in relation to the entire volume.

The black error and white error components were given penalty weights P_{Black}, P_{White} respectively. The error calculation formula is given in (1).

$$error = P_{Black} \cdot error_{Black} + P_{White} \cdot error_{White} \quad (1)$$

Penalty values were initially set to be $P_{Black} = P_{White} = 1$.

The average and standard deviation results for the case of no topological preservation (NTP) and with topological preservation (TP) are presented in Fig. 10. The topological preservation method demonstrates larger errors starting at the fourth LOD. This is due to the constraint which prefers the formation of new bonds and the creation of material over the separation of connected components. However, statistically these two datasets are not significantly different. In order to avoid this misleading result the penalty values were set to be $P_{Black} = 1, P_{White} = 0$, making it acceptable if an element turned from white to black from the original model to a lower LOD. Results for this case are depicted in Fig. 11. It is evident that the error for all LODs is either equal or lower for both methods. Statistical analysis concludes that LODs 4, 5 and 6 of the two methods are significantly different in 95% certainty level.

In conclusion of the statistical analysis, when utilizing topological preservation methods there were less disconnected components and lower volumetric error.

3.4. 3D Examples – Adaptive models

An adaptive model was generated after an ROI was selected based on a curvature criterion. Here we selected the criterion to be a high value of normal curvature. In order to distinguish between different areas of high curvature, non-maximal suppression was used to find local maximum values. Potential ROIs were selected to be the ten vertices with the highest normal curvature with radius of 15% of the model size. The potential ROIs are depicted in Fig. 12, the spheres are semi-transparent and their color corresponds to their curvature value (red is the highest and blue the lowest of the ten). Note that here only some of the spheres are visible because of the point of view.

The bottom center ROI was arbitrarily chosen. The LOD in it was defined to be the maximum inside and minimum outside. The result is depicted in Fig. 13. It can be seen that the local rod feature which includes a ridge that generated the high normal curvature is fully preserved while the rest of the model is coarsely approximated. The color coding here represents the LOD of the elements – red elements are from the highest LOD and blue elements are from the lowest LOD, all other elements color is a linear interpolation between the red and blue.

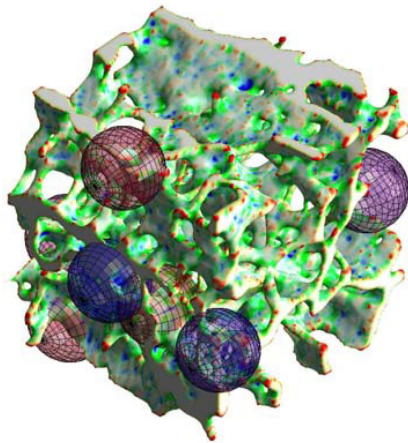


Fig. 12. Bone fragment porous structure with color coded curvature values and potential spherical ROIs based on normal curvature values

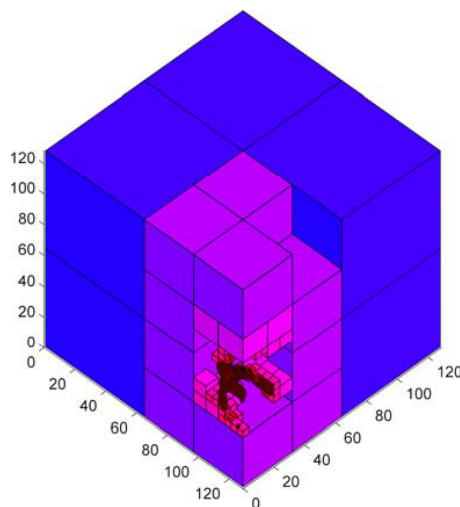


Fig. 13. Porouse micro-structure adaptive model for curvature based ROI selection criterion

4. Summary and Conclusions

An adaptive multi-resolution method for hierarchical volumetric models has been presented. The Octree representation has been applied to the adaptive model. The hierarchical structure was generated and represented in a multi-resolution data structure. The adaptive model was constructed with a mask field. Regions of interest were defined by curvature characteristic and parameters of geometric elements for different LODs.

One of the main advantages of the presented approach is that it enables control over levels of detail for volumetric models and is not limited to a single level. Furthermore, in this paper a certain type of ROI was presented. However, the approach can accommodate for any ROI requirement. There are a few limitations to the approach. The first is the

dependency of the resulted model in the initial orientation, meaning that the same object in different orientations will have different results due to the traversal order on the data structure. In addition, even though a topological preservation method is implemented, there are cases in which the topology will not be completely preserved.

Acknowledgements

The Authors would like to thank Dr. Lev Podshivalov for the bone models and his consulting and support of this work. This study was partially supported by MuProD project under the EU FP7 program.

References

- [1] Samet, H., "The design and analysis of spatial data structures," 1990, Addison-Wesley Reading MA, .
- [2] Samet, H., "Foundations of multidimensional and metric data structures," 2006, Morgan Kaufmann, .
- [3] Gargantini, I., "An Effective Way to Represent Quadrees," *Commun ACM*, 1982, **25**(12) pp. 905-910.
- [4] Podshivalov, L., Fischer, A., and Bar-Yoseph, P., "Multiscale FE Method for Analysis of Bone Micro-Structures," *Journal of the Mechanical Behavior of Biomedical Materials*, 2011, **4**(6) pp. 888-899.
- [5] Podshivalov, L., "3D Hierarchical Geometric Modeling and Multiscale FE Analysis as a Base for Individualized Medical Diagnosis of Bone Structure," 2011, Ph.D thesis, Technion - Israel Institute of Technology, Haifa, Israel, pp. 101.
- [6] Podshivalov, L., Fischer, A., and Bar-Yoseph, P., "3D Hierarchical Geometric Modeling and Multiscale FE Analysis as a Base for Individualized Medical Diagnosis of Bone Structure," *Bone*, 2011, **48**(4) pp. 693-703.
- [7] Ben Shabat, Y., and Fischer, A., "Proceedings of the 24th CIRP Design Conference, Milan, Italy," 2014, Elsevier, .
- [8] Lorensen, W. E., and Cline, H. E., "Marching cubes: A high resolution 3D surface construction algorithm," *ACM Siggraph Computer Graphics*, Anonymous ACM, 1987, **21**, pp. 163-169.
- [9] Desbrun, M., Meyer, M., Schröder, P., "Implicit fairing of irregular meshes using diffusion and curvature flow," *Proceedings of the 26th annual conference on Computer graphics and interactive techniques*, Anonymous ACM Press/Addison-Wesley Publishing Co., 1999, pp. 317-324.
- [10] Rusinkiewicz, S., "Estimating curvatures and their derivatives on triangle meshes," *3D Data Processing, Visualization and Transmission*, 2004. 3DPVT 2004. *Proceedings. 2nd International Symposium on*, Anonymous IEEE, 2004, pp. 486-493.
- [11] Kong, T. Y., and Rosenfeld, A., "Digital Topology: Introduction and Survey," *Computer Vision, Graphics, and Image Processing*, 1989, **48**(3) pp. 357-393.
- [12] Jia, X., Wang, D., Wu, Y., "A shrinking algorithm for binary images to preserve topology," *Image and Signal Processing (CISP)*, 2010 3rd International Congress on, Anonymous IEEE, 2010, **3**, pp. 1181-1185.